agronomy

MDPI

Article

Wheat Yield, Biomass, and Radiation Interception and Utilization Under Conservation Tillage: Greater Response to Drip Fertigation Compared to Intensive Tillage

Yuechao Wang [1,†], Jinxiao Song [2,†], Wen Li [1], Tingting Yan [3], Depeng Wang [2], Jianfu Xue [1,*] and Zhiqiang Gao [1]

[1] College of Agriculture, Shanxi Agricultural University, Jinzhong 030801, China; ycwang@sxau.edu.cn (Y.W.); s20222187@stu.sxau.edu.cn (W.L.); gaozhiqiang1964@sxau.edu.cn (Z.G.)
[2] International School of Bioresource Application, College of Life Science, Linyi University, Linyi 276000, China; songjinxiao@lyu.edu.cn (J.S.); wangdepeng@lyu.edu.cn (D.W.)
[3] Linyi Rural Revitalization Service Center, Linyi 276032, China; tingtingyan84@outlook.com
* Correspondence: fudange95@sxau.edu.cn
† These authors contributed equally to this work.

Abstract: Conservation tillage, particularly no tillage (NT), has been recognized as an efficient farming practice, particularly in dryland agriculture, as it significantly enhances crop yields, improves soil health, and contributes to environmental sustainability. However, the influence of NT on winter wheat radiation interception and utilization, biomass, and yield under NT in irrigated fields, especially under drip fertigation, is unclear. A field experiment was carried out for two growing seasons in Shandong province, China, using a split-plot design with the tillage method as the main plot (no tillage, NT; rotary tillage, RT; and first plowing the soil and then conducting rotary tillage, PRT), and water–nitrogen management as the sub-plot (N fertilizer broadcasting and flood irrigation, BF and drip fertigation, DF). Our results showed that DF increased yield by 11.0–28.5%, but the yield response to DF depended on the tillage methods. NT had the highest response in yield of 26.3–28.5%, followed by RT of 14.6–15.1% and PRT of 11.0–11.9%. Both increased grains per ear and ear number, a result of the greater maximum stems number donating to the yield gain by DF under NT. This gain was also due to the substantially promoted post-anthesis biomass (36.7–47.3%), which resulted from the increased interception of solar radiation and radiation use efficiency after anthesis. In addition, the extended post-anthesis duration also benefited biomass and yield. To conclude, our findings underscore the critical need to optimize water and nitrogen management strategies to maximize yield under conservation tillage systems.

Keywords: drip fertigation; no tillage; yield; biomass; radiation capture; radiation use efficiency

Citation: Wang, Y.; Song, J.; Li, W.; Yan, T.; Wang, D.; Xue, J.; Gao, Z. Wheat Yield, Biomass, and Radiation Interception and Utilization Under Conservation Tillage: Greater Response to Drip Fertigation Compared to Intensive Tillage. *Agronomy* **2024**, *14*, 2849. https://doi.org/10.3390/agronomy14122849

Academic Editor: Andrea Baglieri

Received: 28 October 2024
Revised: 21 November 2024
Accepted: 27 November 2024
Published: 28 November 2024

1. Introduction

Wheat (*Triticum aestivum* L.) is one of the world's most widely grown and consumed cereal crops, serving as a staple food source for billions of people. Its adaptability to diverse climatic conditions makes it crucial for global food security. However, challenges such as growing populations, increased competition for natural resources, and changing climate patterns threaten sustainable wheat production [1]. To balance food production with environmental preservation, sustainable agricultural practices are essential. Among these, conservation tillage, particularly no tillage (NT), has emerged as a promising approach to improve soil health, reduce erosion, and enhance wheat productivity, especially in dryland or rainfed fields where precipitation often falls short of crop needs and irrigation is not feasible [2–5].

However, the effects of NT on wheat yield can be negative in Northern China, where two or more irrigation events are usually conducted at the regreening and/or jointing, booting, and/or anthesis stages because precipitation (100–300 mm) cannot meet the water

demand of high-yield wheat [6–10]. These conflicting outcomes might be due to varying water management practices and experimental regions. A meta-analysis by Zhao [11] found that NT significantly increased yields only in Western Henan, where water scarcity was the main limiting factor for wheat production. In this context, NT effectively conserved moisture and enhanced drought resistance. Conversely, in regions with adequate rainfall or irrigation, the limitations on wheat yield resulting from water scarcity diminished, while the negative impacts of NT, such as poor root penetration and reduced soil aeration, became more pronounced, leading to yield instability across different areas. Another meta-analysis supported this conclusion as well [8]. The yield loss under NT compared to the intensive tillage in irrigated fields mainly came from the lower ear number per unit area, reduced green leaf area index (GLAI), and decreased biomass [8,9,12].

As mentioned above, in irrigated wheat fields, poor root development due to the compact topsoil could limit the absorption of water and nutrients from the subsoil layer under NT, restricting the yield performance of wheat. Therefore, to optimize water and nutrient management strategies to ensure the topsoil holds adequate moisture and nutrient elements, especially the core elements of plant nutrition, nitrogen. Drip fertigation (DF) is an advanced irrigation method that delivers water directly to the plant root zone, improving water-use efficiency and crop productivity [12–14]. DF also promotes the efficient absorption of nitrogen by topsoil roots by applying small and frequent doses of nitrogen fertilizer and reducing water usage during each fertigation event, thereby limiting the downward movement of fertilizer into deeper soil layers [15–18]. Studies have shown that DF can significantly improve the yield of wheat compared to traditional irrigation methods that are characterized by broadcasting N fertilizer and flooding irrigation (BF) [19–21]. The yield advantage of DF over BF was consistently attributed to the enhanced ear number, GLAI, leaf N condition, and post-anthesis biomass [22,23]. Biomass is determined by the intercepted solar radiation (ISR) by the canopy and the efficiency of converting the intercepted radiation into biomass (radiation use efficiency, RUE) [5,24–26]. GLAI plays a core role in capturing radiation [27,28], and RUE is sensitive to the leaf chlorophyll content, especially the flag leaves [29,30]. Tong reported that the increased ISR rather than RUE, contributed to the greater biomass under DF before anthesis compared to BF, whereas the RUE instead of ISR mattered after anthesis under an intensive tillage method [22].

The advantages of DF in enhancing water and nutrient availability in the topsoil show great potential for optimizing GLAI and leaf chlorophyll content. These improvements may enable wheat crops to capture more solar radiation in tandem with increased RUE, leading to greater biomass accumulation and, ultimately, higher grain yields under NT conditions. A field experiment by Chen et al. demonstrated that, under NT, DF with moderate irrigation and NPK inputs outperformed BF with higher levels of irrigation and NPK by increasing the ear number per unit area, resulting in a 21% yield advantage [31]. We hypothesize that DF under NT elicits a more pronounced response in the ear number, GLAI, leaf chlorophyll content, ISR, RUE, biomass, and yield, thus helping to narrow the yield gap between NT and intensive tillage. The specific objectives of this study are to (1) assess the impact of conservation tillage on wheat yield and yield components; (2) quantify the effects of DF on radiation interception, RUE, and biomass production under different tillage methods; and (3) evaluate the compensatory effect of DF on the inferior performance of yield under NT. By addressing these objectives, this study aims to provide insights into the optimal combination of tillage and water–nitrogen management practices to enhance wheat productivity and sustainability, particularly in regions with accessible irrigation.

2. Materials and Methods

2.1. Site Description

Field experiments were conducted at Quanyuan Town (34°42′ N, 118°25′ E, altitude 45 m), Tancheng County, Shandong Province, in two winter wheat growing seasons during 2022–2023 and 2023–2024. The site has a typical temperate monsoon climate (Köppen classification). The dominant cropping system is winter wheat and summer corn rotation.

The local farmers usually carry out no-till direct seeding of summer corn after the wheat harvest. Summer corn is harvested using large combine harvesters, and the harvesting and transportation of corn ears will compact the soil layer. Therefore, farmers usually perform rotary tillage before wheat sowing or deep plowing before rotary tillage. Experiments were conducted in two closely adjacent fields in the two growing seasons. The previous crop was summer corn with normal and uniform management (similar to local farmers planting a single corn cultivar, applying 240 kg N ha^{-1}, 150 kg P_2O_5 ha^{-1}, and 120 kg K_2O ha^{-1}, irrigating twice after planting and at silking with 60 mm per dose). Nine replicate soil samples were randomly collected from the 0–20 cm soil layer for soil analysis before applying the basal fertilizer in 2022 and 2023. The soil type was classified as silty clay loam according to the USDA soil taxonomy, with a pH of 8.14–8.20, organic matter content of 16.77–17.26 g kg^{-1}, total N content of 0.84–0.91 g kg^{-1}, alkaline N content of 44.36–46.23 mg kg^{-1}, Olsen P content of 17.87–18.69 mg kg^{-1}, and available K content of 141.36–150.85 mg kg^{-1} in 0–20 cm soil.

The climate parameters, comprising the daily minimum temperature, maximum temperature, incident solar radiation, and precipitation during the growing period from sowing to maturity in both seasons, were collected from a weather station (AWS 800, Campbell Scientific, Inc., Logan, UT, USA) located about 150 m from the experimental field. The developmental stages of the wheat plants were recorded using the Zadoks scale. The seasonal average daily mean temperature, total precipitation, and incident solar radiation in the growing seasons during 2022–2023 and 2023–2024 were 10.93 °C and 10.74 °C, 407.9 mm and 221.9 mm, and 2850 MJ m^{-2} and 2942 MJ m^{-2}, respectively (Figure 1).

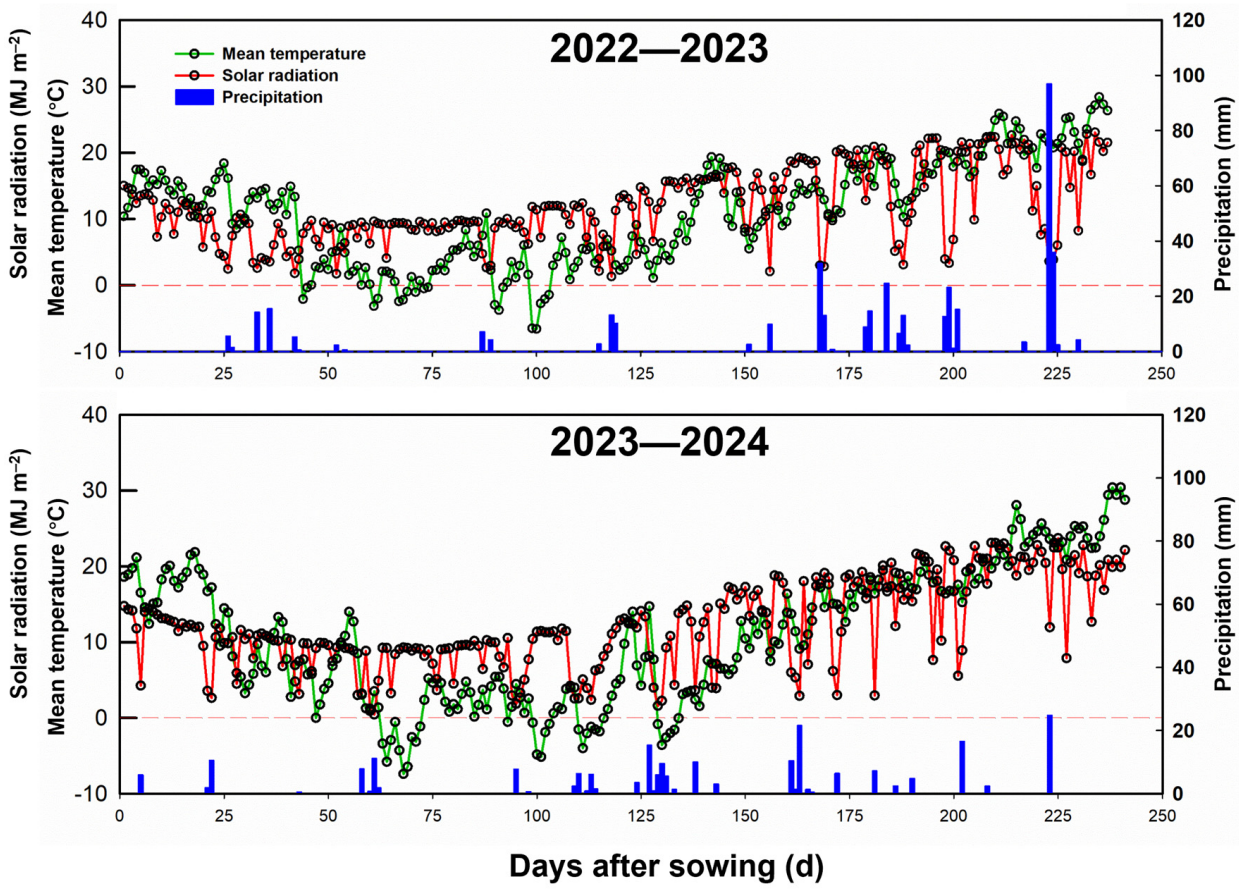

Figure 1. Daily mean temperature, solar radiation, and precipitation recorded from sowing to maturity in 2022–2023 and 2023–2024 growing seasons.

2.2. Experimental Design and Crop Management

The treatments were arranged in a split-plot design with four replicates. The soil tillage method was designated as the main plot and water–nitrogen management (WN) as the sub-plot. Each subplot measured 25.0 m in length and 2.25 m in width. The tillage method comprised no tillage (NT), rotary tillage with a depth of 15 cm (RT), and the conventional tillage method commonly adopted by local farmers in the area, namely first plowing the soil with a depth of 30 cm and then conducting rotary tillage (PRT). The WN comprised conventional management, N fertilizer broadcast and flood irrigation (BF), and drip fertigation (DF). The widely planted wheat cultivar Jimai22 was used. The sowing was conducted with a no-tillage wheat planter, (2BMF-11; Minle County Kaiyuan Machinery Manufacturing Co., Ltd., Minle, Gansu, China). The planter had 11 sowing ports, but the one on the far right had been removed before working. Therefore, there were 10 rows in each plot and the row space was 20 cm. The predetermined seed rate was 450 seeds m^{-2}.

The harvest time for the previous crop is 11 October and 8 October in 2022 and 2023, respectively. When the corn was harvested, the harvester crushed the straw into fragments with a length of no more than 5 cm, which were evenly scattered on the soil surface. The wheat crops were sowed on 17 October and 14 October in 2022 and 2023, respectively.

Before sowing, phosphate, in the form of calcium super-phosphate (16% P_2O_5), was applied at 150 kg P_2O_5 ha^{-1}, and potassium, in the form of potassium chloride (52% K_2O), was applied at 90 kg K_2O ha^{-1}. N fertilizer was applied as urea (46% N). The total N rate for all treatments was 250 kg N ha^{-1}. For BF, the topdressing N fertilizer was broadcasted into the plot first, and then, flooding irrigation of 60 mm was conducted at the jointing stage (Zadoks code 32). Before winter, at the heading (Zadoks code 50) and the early milk (Zadoks code 73, only in 2024) stages, flooding irrigation of 60 mm was carried out. For DF, the drip fertigation system was installed at the time when 4 leaves unfolded (Zadoks code 14). For DF, all the irrigation was completed through a drip fertigation system. The drip tapes (Φ 16 mm) were arranged 40 cm apart, with one drip line serving two rows of winter wheat, and the dripper spacing was 30 cm. The drippers discharged 2.4 L h^{-1} at a working pressure of 0.10–0.15 MPa. A flow meter was placed in each plot to monitor the amount of irrigation water released. At the regreening, jointing, booting, and heading stages, the weighed urea was dissolved into the fertilizer tank, and a Venturi fertilizer applicator was used to suck the fertilizer into the pipeline. Then, it was dripped into the field with drip tapes. The same amount of water was added to the fertilization tanks in each plot. Irrigation and N fertilization management were conducted as described in Table 1. The field was kept free of diseases, pests, and weeds.

Table 1. Irrigation and N fertilizer management.

Season	WN	Irrigation Management (mm)								N Management (kg ha^{-1})					
		BW	**RS**	**JS**	**BS**	**HS**	**AS**	**EM**	**Total**	**Basal**	**RS**	**JS**	**BS**	**HS**	**Total**
2022–2023	BF	60		60		60			180	150		100			250
	DF	60	30	30	30	30			180	100	25	75	25	25	250
2023–2024	BF	60		60		60		60	240	150		100			250
	DF	60	30	30	30	30	30	30	240	100	25	75	25	25	250

BW, before winter. RS, regreening stage. JS, jointing stage. BS, booting stage. AS, anthesis stage. EM, early milk stage. HS, heading stage.

2.3. Sampling and Measurements

The maximum number of stems (sum of main stems and tillers) was counted in five typical and central rows over a length of 1 m (1.00 m^2) at jointing. The productive stems percentage was calculated as the ratio of the ears number at maturity (Zadoks code 91) to the maximum number of stems at jointing. At anthesis and every 7 days after anthesis, the relative chlorophyll content (SPAD value) of 10 typical flag leaves was measured by a chlorophyll meter (HT-YLS, Jingcheng Huatai, Beijing, China), and the wheat plants were

sampled from a typical and central row over a length of 0.5 m (0.125 m^2). The green leaves were separated and measured using a leaf area meter (LI-3100C, LI-COR, Lincoln, NE, USA), before calculating the GLAI, as follows.

$$\text{GLAI}(m^2m^{-2}) = \frac{\text{Green leaf area}}{\text{Sampled land area}}$$

At anthesis, the dry weights of whole plants were measured after oven drying to a constant weight at 80 °C to determine the pre-anthesis biomass. At maturity, the plants sampled from a typical central row over a length of 0.5 m (0.10 m^2) were manually divided into grain and straw. Dry weights were measured for the grain and straw after oven drying to a constant weight at 80 °C. The total biomass at maturity was the total dry weight of the grain and straw. The post-anthesis biomass and the translocated biomass ($\text{Biomass}_{\text{trans}}$) from vegetative organs to grains were calculated as follows.

$$\text{Post-anthesis biomass} = \text{Total biomass} - \text{Pre-anthesis biomass}$$

$$\text{Biomass}_{\text{trans}} = \text{Yield} \times 0.87 - \text{Post-anthesis biomass}$$

where 0.87 represents the proportion of dry matter to the grain yield.

The contribution rates of post-anthesis biomass and translocated biomass to grain yield (CRG_{post} and $\text{CRG}_{\text{trans}}$) were calculated as follows.

$$\text{CRG}_{\text{post}}(\%) = \frac{\text{Post-anthesis biomass}}{\text{Yield} \times 0.87} \times 100$$

$$\text{CRG}_{\text{trans}}(\%) = \frac{\text{Biomass}_{\text{trans}}}{\text{Yield} \times 0.87} \times 100$$

The harvest index (HI) was calculated as follows.

$$\text{HI}(\%) = \frac{\text{Yield} \times 0.87}{\text{Total biomass}} \times 100$$

At maturity, wheat ears were cut from an area of 2.0 m^2 (length of 2.00 m in five typical rows) in the center of each plot, and the number of productive ears that produced at least five grains was recorded. The grain yield was adjusted to a standard moisture content of 0.130 g H_2O g^{-1} fresh weight. The grain moisture content was measured using a digital moisture tester (PM8188A, Kett Electric Laboratory, Tokyo, Japan). Three sub-samples weighing 50.00 g were taken from the grain samples to count the number of grains and calculate the grain weight, which was also adjusted to a moisture content of 13.0%. The number of grains per ear was calculated as follows.

$$\text{Grains per ear} = \frac{\text{Grain yield}}{\text{Grain weight} \times \text{Ears number}}$$

Canopy PAR interception was measured during the growing seasons. The measurements were performed between 1100 h and 1300 h at an interval of 7–15 days using a linear PAR ceptometer (AccuPAR LP-80, Decagon Devices Inc., Pullman, WA, USA). In each plot, the transmitted PAR intensity was measured by placing the light bar vertically to rows and slightly above the soil surface. The PAR intensity above the canopy (PAR_a) was recorded immediately after measuring the transmitted PAR intensity (PAR_t). Six pairs of PAR intensity measurements were recorded below and above the canopy. The canopy PAR interception ratio (PARI) was calculated as follows.

$$\text{PARI}(\%) = \frac{\text{PAR}_a - \text{PAR}_t}{\text{PAR}_a} \times 100$$

The intercepted solar radiation (ISR) during a growth period was calculated using the average canopy PARI and accumulated incident solar radiation in the growth period as follows.

$$\mathrm{ISR}\left(\mathrm{MJm}^{-2}\right) = \frac{\text{PARI at the beginning} + \text{PARI at the end of the period}}{2} \times \text{incident solar radiation}$$

The ISR during the entire growing season was the summed ISR during each growth period. The RUE during one period was calculated as follows.

$$\mathrm{RUE}(\mathrm{gMJ}^{-1}) = \frac{\text{Biomass}}{\text{ISR}}$$

2.4. Data Analysis

Statistical analyses were performed with Statistix 9.0 (Analytical Software, Tallahassee, FL, USA). Normality and homogeneity of variance were checked using the Shapiro–Wilk test and Levene test, respectively, which indicated that the general linear model could be used to conduct an analysis of variance and multiple comparisons without data transformations. An analysis of variance was conducted separately each year. Differences in traits under NT, RT, and PRT at the specific WN were detected using the least significant difference test (α = 0.05). A Pearson correlation analysis was conducted to determine the correlation coefficient (r) and p-value. All graphical representations of the data were produced using SigmaPlot 12.5 (Systat Software Inc., Point Richmond, CA, USA).

3. Results

3.1. Growth Duration

Both tillage and WN had an obvious influence on the growth duration of winter wheat (Table 2). In both seasons, all of the tillage methods showed longer durations of sowing–anthesis and anthesis–maturity under DF than BF. As a result, DF extended the durations of sowing–maturity by 3 to 7 days over BF. The NT displayed a shorter duration than RT and PRT for all growth phases under both WNs and in both seasons, except for the anthesis–maturity phase under DF in the 2023–2024 season.

Table 2. Growth duration of winter wheat.

Season	Tillage	WN	From Sowing to Anthesis (d)	From Anthesis to Maturity (d)	From Sowing to Maturity (d)
2022–2023	NT	BF	190	39	229
		DF	192	42	234
	RT	BF	193	40	233
		DF	193	44	237
	PRT	BF	193	41	234
		DF	193	44	237
2023–2024	NT	BF	193	39	232
		DF	195	44	239
	RT	BF	195	41	236
		DF	197	44	241
	PRT	BF	195	43	238
		DF	197	44	241

3.2. Yield and Yield Components

Both the tillage method and the WN had significant effects on yield in both seasons (Table 3). Averaged across two WNs, the PRT produced 16.5–17.1% and 10.8–10.9% higher yields than NT and RT, respectively. The yield difference among the tillage methods mainly came from ear numbers. The average ear number of PRT was 19.7–20.2% and 11.7–13.1% greater than NT and RT, respectively. Compared to ear number, grain per ear was less

responsive to the tillage method. Averaged across three tillage methods, DF outyielded BF by 16.8% and 17.8% in 2022–2023 and 2023–2024, respectively. The improved yield by DF was mainly attributed to the increased grains per ear (8.6–8.8%) and ear number (5.0–5.9%).

Table 3. Yield and yield components of winter wheat.

Season	Tillage	WN	Yield (t ha^{-1})	Ear Number (10^4 ha^{-1})	Grain per Ear	Grain Weight (mg)
2022–2023	NT	BF	8.20 d	514 c	31.8 c	50.3 ab
		DF	10.36 b	584 b	34.7 ab	51.1 a
	RT	BF	9.09 c	578 b	32.0 c	49.1 b
		DF	10.44 b	599 b	35.0 ab	49.9 ab
	PRT	BF	10.24 b	651 a	33.3 bc	47.3 c
		DF	11.37 a	662 a	36.1 a	47.6 c
	MEAN	NT	9.28 C	549 C	33.2 B	50.7 A
		RT	9.76 B	588 B	33.5 AB	49.5 AB
		PRT	10.81 A	657 A	34.7 A	47.4 B
		BF	9.18 B	581 B	32.4 B	48.9 A
		DF	10.72 A	615 A	35.2 A	49.5 A
	ANOVA	T	**	**	*	**
		WN	**	**	**	ns
		T × WN	**	**	ns	ns
2023–2024	NT	BF	7.51 d	537 c	30.9 e	45.2 b
		DF	9.65 b	602 b	33.9 bc	47.3 a
	RT	BF	8.43 c	593 b	32.1 de	44.2 bc
		DF	9.70 b	616 b	34.6 ab	45.5 b
	PRT	BF	9.49 b	682 a	32.9 cd	42.3 d
		DF	10.62 a	685 a	35.9 a	43.1 cd
	MEAN	NT	8.58 C	569 C	32.4 B	46.3 A
		RT	9.06 B	605 B	33.4 AB	44.8 B
		PRT	10.05 A	684 A	34.4 A	42.7 C
		BF	8.48 B	604 B	32.0 B	43.9 B
		DF	9.99 A	634 A	34.8 A	45.3 A
	ANOVA	T	**	**	*	**
		WN	**	**	**	*
		T × WN	**	**	ns	ns

*, **, significant at 0.05 and 0.01 probability levels, respectively; ns, not significant at 0.05 probability level. Different uppercase letters indicate a significant difference between the means of WNs across three tillage methods or between tillage methods across two WNs according to the least significant difference test (α = 0.05). Within a column and a season, different lowercase letters indicate significant differences between treatments (tillage method combined WN) according to the least significant difference test (α = 0.05).

The response of yield to WN varied across tillage methods, which was evidenced by the fact that the interactive effect between tillage and WN (T × WN) on grain yield was significant (Table 3). The yield gain by DF for NT was 26.3–28.5%. The corresponding gain percentages for RT and PRT were 14.6–15.1% and 11.0–11.9%, respectively. The improved ear number per hectare (12.1–13.6%) and grain per ear (9.1–9.7%) by DF -could explain the substantial yield gain for NT under DF. However, the yield gains for RT and PRT were only attributed to the improved grains per ear of 7.8–9.4% and 8.4–9.1%, respectively.

3.3. Population Size and Individual Productivity

The average maximum stem number under DF was 6.3–6.8% greater than BF (Table 4). Significantly lower productive stem percentages were observed for PRT than for NT and RT. Although the simple effect of WN on the productive stem percentage was not significant, a significant interactive effect between the tillage method and WN was observed. In both seasons, DF slightly increased the productive stem percentage of NT by 3.1–4.7% ($p > 0.05$), but a reduction by DF occurred for RT and PRT. The yield per ear did not

significantly respond to the tillage method. However, the yields per ear were consistently and significantly improved by DF for all tillage methods.

Table 4. Maximum stem number, productive stem percentage, and yield per ear of winter wheat.

Season	Tillage	WN	Maximum Stem Number (10^4 ha^{-1})	Productive Stem Percentage (%)	Yield per Ear (g)
2022–2023	NT	BF	1336 d	38.5 ab	1.60 b
		DF	1451 c	40.3 a	1.77 a
	RT	BF	1471 c	39.3 a	1.57 b
		DF	1587 b	37.7 b	1.74 a
	PRT	BF	1826 a	35.7 c	1.57 b
		DF	1907 a	34.7 c	1.72 a
	MEAN	NT	1394 C	39.4 A	1.68 A
		RT	1529 B	38.5 A	1.66 A
		PRT	1867 A	35.2 B	1.65 A
		BF	1544 B	37.8 A	1.58 B
		DF	1649 A	37.6 A	1.74 A
	ANOVA	T	**	**	ns
		WN	**	ns	**
		T × WN	**	**	**
2023–2024	NT	BF	1283 d	41.8 ab	1.40 b
		DF	1396 c	43.1 a	1.60 a
	RT	BF	1421 c	41.8 ab	1.42 b
		DF	1531 b	40.2 b	1.57 a
	PRT	BF	1769 a	38.6 bc	1.39 b
		DF	1829 a	37.4 c	1.55 a
	MEAN	NT	1340 C	42.5 A	1.50 A
		RT	1476 B	41.0 A	1.50 A
		PRT	1799 A	38.0 B	1.47 A
		BF	1491 B	40.7 A	1.40 B
		DF	1585 A	40.3 A	1.58 A
	ANOVA	T	**	**	ns
		WN	**	ns	**
		T × WN	ns	**	ns

**, significant at 0.01 probability level; ns, not significant at 0.05 probability level. The data of seedling number and emergence rate had been counted and calculated at 3-leaf stage when the WN was not conducted. Different uppercase letters indicate a significant difference between the means of WNs across three tillage methods or between tillage methods across two WNs according to the least significant difference test (LSD, $\alpha = 0.05$). Within a column and a season, different lowercase letters indicate significant differences between treatments (tillage method combined WN) according to the least significant difference test (LSD, $\alpha = 0.05$).

3.4. Biomass Production, Translocation and Partitioning

Both the tillage method and WN had significant effects on biomass production (pre-anthesis, post-anthesis, and total biomass) (Table 5). DF increased the average pre-anthesis, post-anthesis, and total biomass by 12.6–12.7%, 28.3–31.2%, and 18.7–19.4%. Notably, the responses of biomass to DF significantly varied among tillage methods. DF increased the total biomass for NT, RT, and PRT by 26.8–26.9%, 16.5–16.8%, and 14.3–14.4%, respectively. For pre-anthesis biomass, the corresponding percentages were 20.6–21.2%, 7.1–8.5%, and 9.6–11.0%, and for post-anthesis, they were 36.7–47.3%, 31.9–32.0%, and 19.4–21.9%.

Table 5. Biomass production, translocation, and partitioning of winter wheat.

Season	Tillage	WN	Pre-B (t ha^{-1})	Post-B (t ha^{-1})	Total-B (t ha^{-1})	Trans-B (t ha^{-1})	CRG_{Post} (%)	CRG_{Trans} (%)	HI (%)
2022–2023	NT	BF	9.01 d	5.51 e	14.52 d	1.63 a	77.2 d	22.8 a	49.2 a
		DF	10.87 bc	7.53 c	18.41 b	1.48 a	83.5 c	16.5 b	48.9 a
	RT	BF	10.23 c	6.15 d	16.38 c	1.76 a	77.8 d	22.2 a	48.3 ab
		DF	10.96 b	8.12 b	19.09 b	0.96 b	89.4 b	10.6 c	47.6 ab
	PRT	BF	11.23 b	7.88 bc	19.11 b	1.03 b	88.5 b	11.5 c	46.6 bc
		DF	12.46 a	9.41 a	21.87 a	0.48 c	95.1 a	4.9 d	45.3 c
	MEAN	NT	9.95 C	6.51 C	16.47 C	1.56 A	80.4 C	19.6 A	49.0 A
		RT	10.60 B	7.14 B	17.74 B	1.36 A	83.6 B	16.4 B	47.9 AB
		PRT	11.84 A	8.65 A	20.49 A	0.76 B	91.8 A	8.2 C	45.9 B
		BF	10.16 B	6.51 B	16.67 B	1.47 A	81.1 B	18.9 A	48.0 A
		DF	11.44 A	8.35 A	19.79 A	0.98 B	89.4 A	10.6 B	47.3 A
	ANOVA	T	**	**	**	**	**	**	*
		WN	**	**	**	**	**	**	ns
		T × WN	**	**	**	**	**	**	ns
2023–2024	NT	BF	8.44 d	4.53 c	12.98 d	2.00 a	69.4 d	30.6 a	50.4 a
		DF	10.23 bc	6.51 b	16.74 b	1.88 ab	77.6 c	22.4 b	50.2 a
	RT	BF	9.64 c	5.31 b	14.96 c	2.02 a	72.5 d	27.5 a	49.1 ab
		DF	10.46 bc	7.01 b	17.48 b	1.42 cd	83.1 b	16.9 c	48.3 bc
	PRT	BF	10.86 b	6.58 a	17.44 b	1.68 bc	79.6 c	20.4 b	47.4 bc
		DF	11.93 a	8.02 a	19.95 a	1.21 d	86.9 a	13.1 d	46.3 c
	MEAN	NT	9.33 C	5.52 C	14.86 C	1.94 A	73.5 C	26.5 A	50.3 A
		RT	10.05 B	6.16 B	16.22 B	1.72 AB	77.8 B	22.2 B	48.7 AB
		PRT	11.39 A	7.30 A	18.69 A	1.45 B	83.3 A	16.7 C	46.8 B
		BF	9.65 B	5.48 B	15.12 B	1.90 A	73.8 B	26.2 A	48.9 A
		DF	10.87 A	7.18 A	18.06 A	1.51 B	82.5 A	17.5 B	48.2 A
	ANOVA	T	**	**	**	**	**	**	*
		WN	**	**	**	**	**	**	ns
		T × WN	**	**	**	**	**	**	ns

Pre-B, pre-anthesis biomass; Post-B, post-anthesis biomass; Total-B, total biomass; Trans-B, translocated biomass; CRG_{Post}, the contribution rate of post-anthesis biomass to grain yield; CRG_{Trans}, the contribution rate of translocated biomass to grain yield; HI, harvest index. *, **, significant at 0.05 and 0.01 probability levels, respectively; ns, not significant at 0.05 probability level. Different uppercase letters indicate a significant difference between the means of WNs across three tillage methods or between tillage methods across two WNs according to the least significant difference test ($\alpha = 0.05$). Within a column and a season, different lowercase letters indicate significant differences between treatments (tillage method combined WN) according to the least significant difference test ($\alpha = 0.05$).

Biomass translocation was significantly affected by the tillage method and WN, as well as their interaction (Table 5). The average biomass translocation under BF was 25.8–50.0% greater than DF. There was no significant difference in biomass translocation for NT between BF and DF in either season. However, 42.3–83.2% and 38.8–114.6% higher biomass translocations were achieved under BF than DF for RT and PRT, respectively. The highest average CRG_{Post} was achieved at PRT (83.3–91.8%), followed by RT (77.8–83.6%) and NT (73.5–80.4%). The performance of CRG_{Trans} was the opposite. Only the tillage method had a significant effect on HI, and the response of HI was relatively weak compared to biomass.

A Pearson correlation analysis showed that the yield was significantly related to the post-anthesis biomass ($r^2 \geq 0.9659$, $p < 0.01$) in both seasons, whereas a significant relationship between yield and biomass translocation ($r^2 \geq 0.7036$, $p < 0.05$) was observed (Figure 2). In addition, there was a significantly negative relationship between biomass translocation and post-anthesis biomass ($r^2 \geq 0.8248$, $p < 0.05$) in both seasons.

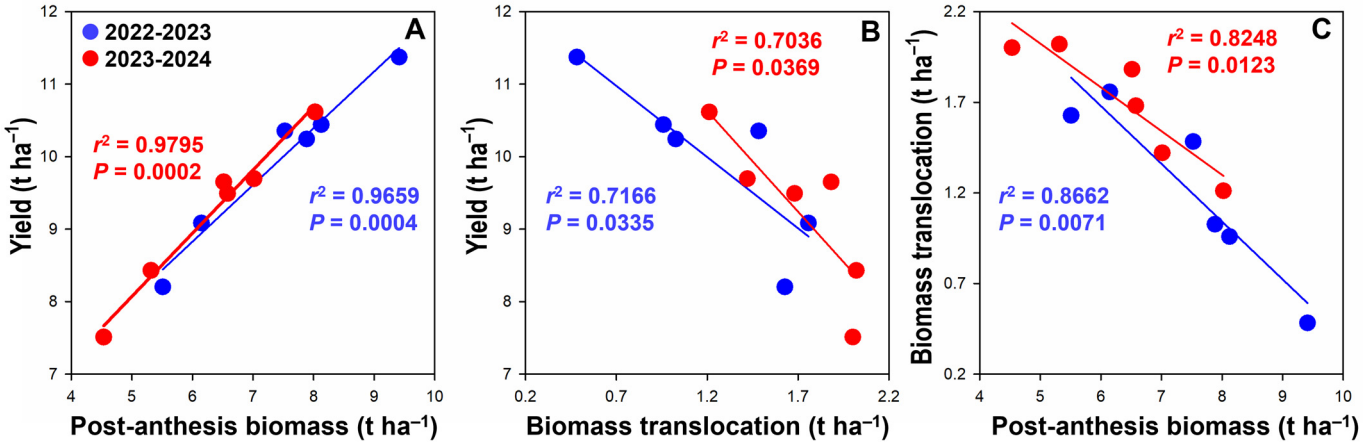

Figure 2. The relationship between yield and post-anthesis biomass (**A**), between yield and biomass translocation (**B**), and between biomass translocation and post-anthesis biomass (**C**). For each season, n = 6.

3.5. Radiation Interception and Use Efficiency

The tillage method and WN, as well as their interaction, significantly affected the ISR in both seasons (Figure 3). DF increased the averaged pre-anthesis, post-anthesis, and total ISR by 3.4–4.8%, 16.5–16.8%, and 14.3–14.4% for NT, RT, and PRT, respectively. However, the effect of WN on ISR depended on the tillage method. For pre-anthesis ISR, significant increases (7.3–10.1%) by DF were achieved only for NT in both seasons. For the post-anthesis ISR, increases for NT, RT, and PRT were 16.1–20.7%, 12.0–12.1%, and 4.8–9.6%, respectively. For the total ISR, the corresponding percentages were 10.5–14.3%, 5.2–6.6%, and 3.1($p > 0.05$, 2023–2024)–4.9%.

All pre-anthesis, post-anthesis, and seasonal RUE were significantly affected by the tillage method, WN, and their interaction (T × WN) (Figure 4). Averaged across tillage methods, the pre-anthesis, post-anthesis, and seasonal RUE were increased by 7.7–8.9%, 14.4–17.7%, and 11.1–11.4% under DF, respectively. Notably, the effect degree of WN on RUE varied among the tillage methods. Before anthesis, increases in RUE by DF of 10.0–12.7%, 5.5–5.9%, and 7.8–8.5% were obtained for NT, RT, and PRT, respectively. After anthesis, the corresponding gain percentages were 17.6–19.1%, 17.7–18.0%, and 9.0–16.4%, and for the seasonal RUE, the values were 12.9–14.8%, 9.6–10.8%, and 9.0–11.0%.

3.6. Dynamics of GLAI and Flag Leaf Relative Chlorophyll Content (SPAD) After Anthesis

Generally, DF had a positive effect on GLAI and SPAD throughout the post-anthesis phase for all tillage methods (Figures 5 and 6). At anthesis, significant increases (13.1–13.7%) in GLAI by DF were achieved only for NT in both seasons. From the 7th to the 35th day after anthesis, significantly higher GLAIs were observed under DF for both NT and RT. However, inconsistent observations across the measuring dates occurred after anthesis for PRT in both seasons. In addition, there were obvious differences in the improvements in GLAI by DF throughout the post-anthesis phase. In descending order, they were NT, RT, and PRT.

From the 7th to the 35th days after anthesis, the flag leaf SPAD value was significantly increased by DF over BF for NT and RT in both seasons. Whereas the statistical significance of the positive effect of DF on SPAD was inconsistent among the measuring dates and seasons. Similar to GLAI, obviously the highest improvements in SPAD by DF throughout the post-anthesis phase were achieved for NT, followed by RT and PRT. Notably, the SPAD displayed a slight increase or stability from anthesis to the 7th day after anthesis under DF, which was in contrast to the obvious continuous decrease of SPAD under BF.

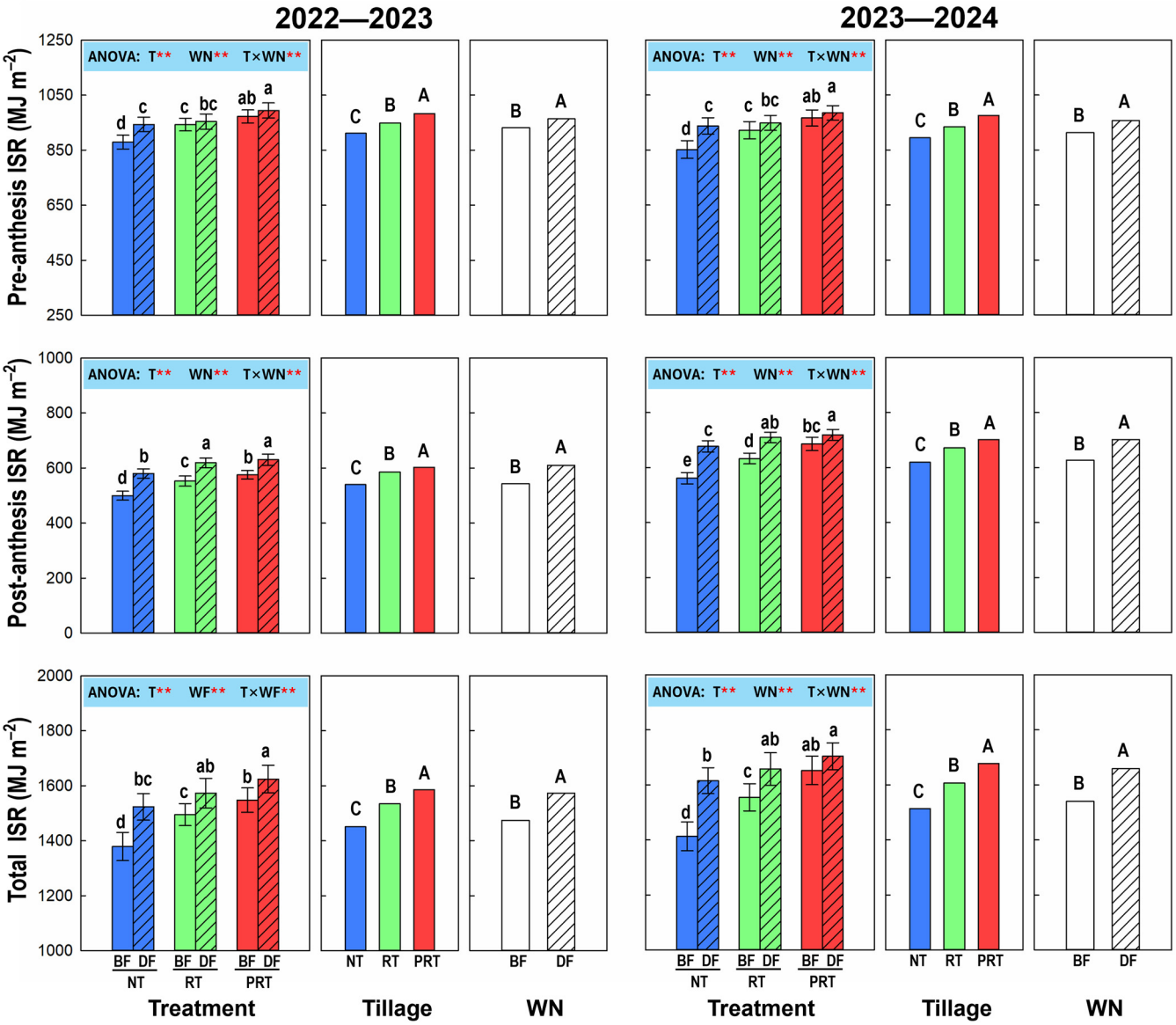

Figure 3. Intercepted solar radiation (ISR) of winter wheat. Data are means and error bars are SE (n = 4). **, significant at 0.01 probability level. Different uppercase letters indicate that there is a significant difference between the means of WNs across three tillage methods or between the means of tillage methods across two WNs according to the least significant difference test ($\alpha = 0.05$). Different lowercase letters indicate there is a significant difference between treatments (tillage method combined with WN) according to the least significant difference test ($\alpha = 0.05$).

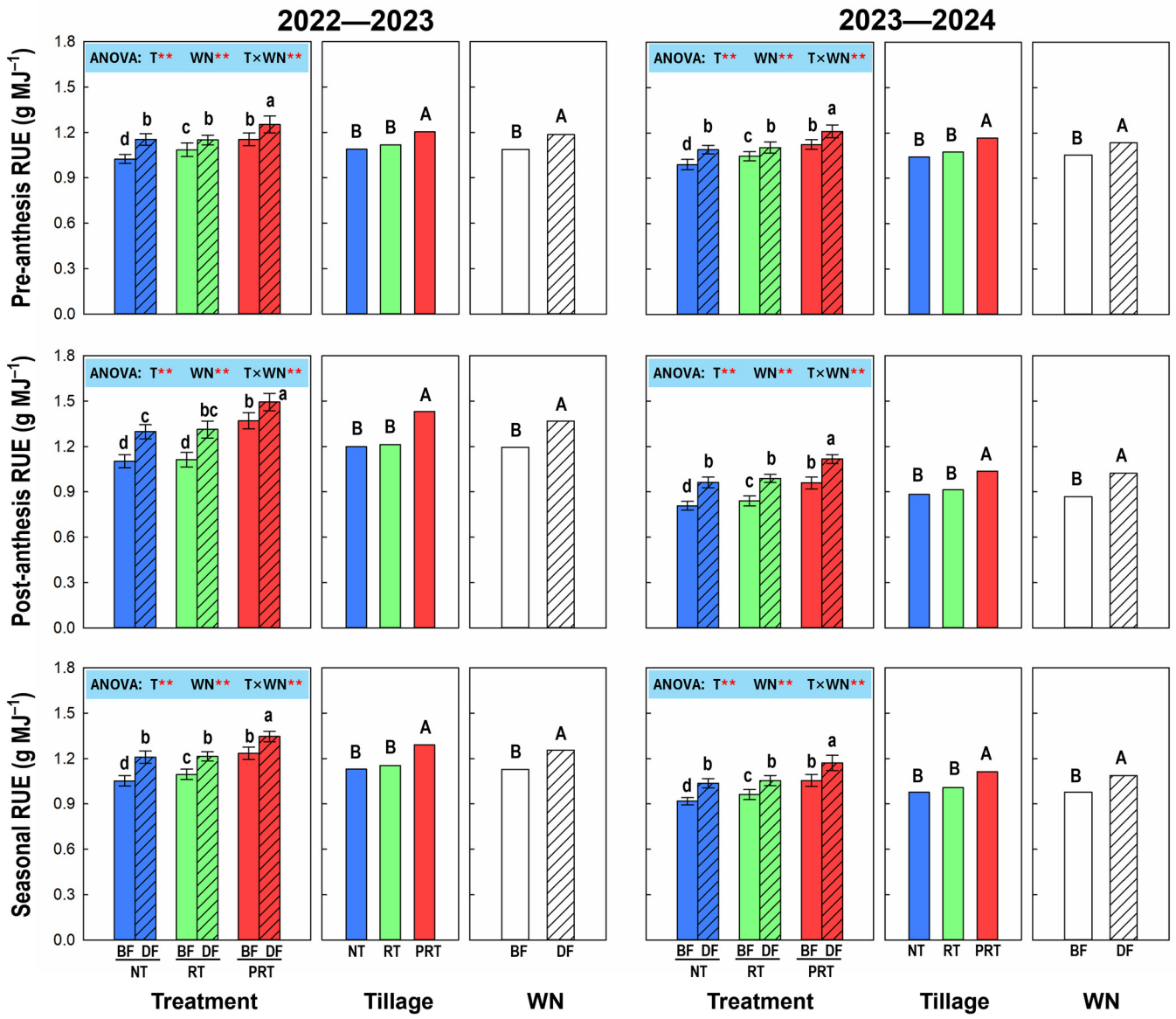

Figure 4. Radiation use efficiency (RUE) of winter wheat. Data are means and error bars are SE (n = 4). **, significant at 0.01 probability level. Different uppercase letters indicate that there is a significant difference between the means of WNs across three tillage methods or between the means of tillage methods across two WNs according to the least significant difference test (α = 0.05). Different lowercase letters indicate there is a significant difference between treatments (tillage method combined with WN) according to the least significant difference test (α = 0.05).

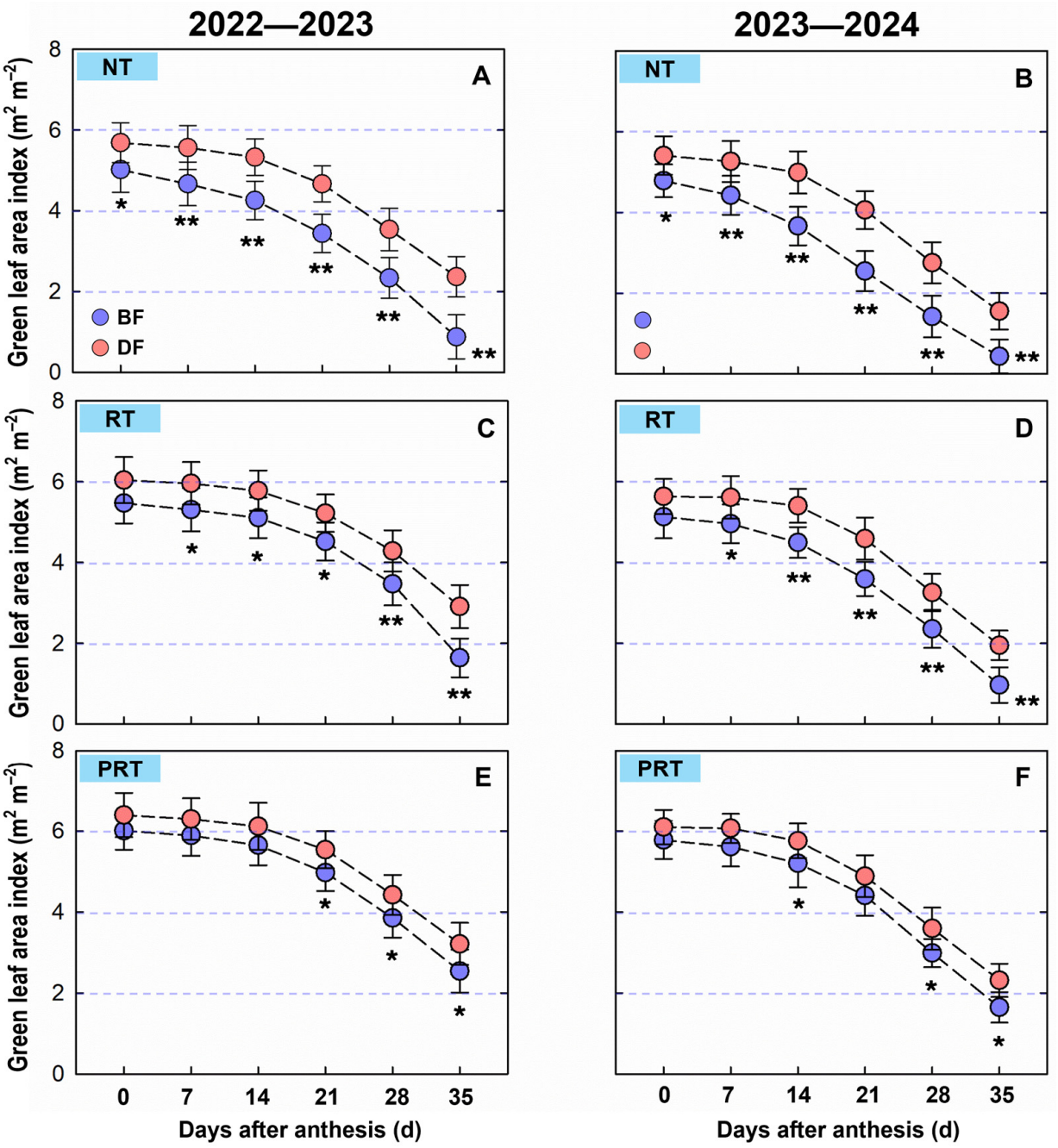

Figure 5. Dynamics of green leaf index after anthesis under NT (**A**,**B**), RT (**C**,**D**) and PRT (**E**,**F**). * and ** indicate that there is a significant difference between WNs under a specific tillage method according to the least significant difference test at α = 0.05 and 0.01, respectively.

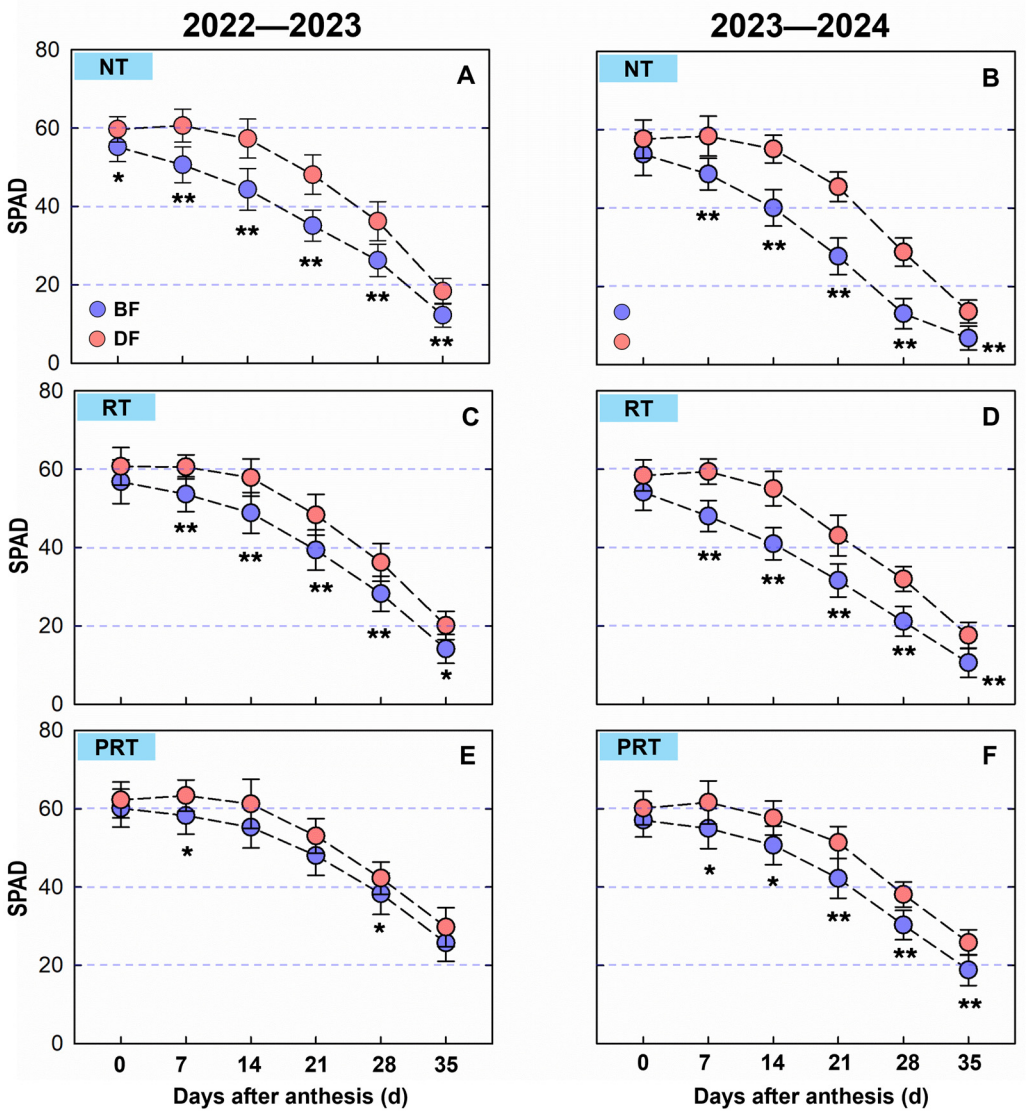

Figure 6. Dynamics of relative chlorophyll content (SPAD) after anthesis under NT (**A**,**B**), RT (**C**,**D**) and PRT (**E**,**F**). * and ** indicate that there is a significant difference between WNs under a specific tillage method according to the least significant difference test at α = 0.05 and 0.01, respectively.

4. Discussion

It is widely recognized that tillage methods and water–nitrogen management significantly influence wheat crop yields [6,19,31–33]. Numerous studies conducted under dryland conditions have concluded that conservation tillage, particularly no tillage (NT), often outperforms intensive tillage due to its ability to conserve soil moisture, increase organic matter content, and reduce evaporation losses [2,3,8,34]. However, in regions with sufficient rainfall or irrigation, intensive tillage was shown to produce higher wheat yields by enhancing nutrient availability and promoting root growth [6,7,12]. Our results showed that, under conventional water–nitrogen management (BF), NT produced the lowest yields (7.51–8.20 t ha^{-1}) among the three tillage methods, yielding 19.9–20.9% less than intensive tillage (PRT). In contrast, DF had a positive effect on wheat yield, improving it by 11.0–28.5%, which aligned with the findings from previous studies [23,35]. Importantly, the yield response to DF varied by tillage method, with NT showing the highest yield increase of 2.14–2.16 t ha^{-1} (26.3–28.5%), followed by RT at 1.27–1.35 t ha^{-1} (14.6–15.1%) and PRT at 1.12–1.13 t ha^{-1} (11.0–11.9%). As a result, under DF, the yield of NT reached 9.65–10.36 t ha^{-1}, which was only 8.9–9.1% lower than PRT. These findings suggest that DF

can significantly enhance the yield performance of conservation tillage while benefiting the environment and ecology.

The yield disadvantage of NT under BF compared to RT and PRT was primarily due to a reduced ear number, a result of the decreased maximum stem number. Similar conclusions were drawn in studies by Chen et al., Guan et al. and Liu et al. [10,36,37]. A meta-analysis also reported that the yield decrease by NT was attributed to the decreased ear number in North China [8]. Nitrogen is a critical factor influencing the development of both the stem and spikelet in wheat ears [38–40]. Research has consistently shown that DF improves N availability in the topsoil, enhancing N absorption and utilization by crops [15–17]. The replacement of BF with DF resulted in an increase in grains per ear across all tillage methods, but an increase in ear number was observed only for NT. These gains in ear number and grains per ear contributed to the highest yield response for NT to DF. These results encouraged us to reasonably assume that NT could not ensure that the wheat plants acquire sufficient nutrients to produce a suitable number of stems compared to RT and PRT, even given the same water and nutrient inputs under BF. This underscores the need to optimize water–nitrogen management strategies to enhance wheat productivity in conservation tillage systems. Future research should investigate the extent to which DF improves soil N availability and plant N assimilation, particularly during the critical stages of stem and spikelet development under different tillage methods.

The mass in grain has two sources, namely the biomass production after anthesis and the translocation of carbohydrates temporarily stored in vegetative organs before anthesis [41–43]. High post-anthesis biomass and biomass translocation are both needed for achieving a high yield [44]. In this study, post-anthesis biomass accounted for 69.4–95.1% of the yield. This result indicated that the wheat yield mainly depended on the post-anthesis biomass, which was evidenced by the high coefficient of the linear relationship between the yield and the post-anthesis biomass ($r^2 \geq 0.9659$, $p < 0.01$. Figure 2A). For all tillage methods, DF increased the post-anthesis biomass by 1.44–2.02 t ha^{-1}, i.e., by an increased percent of 19.4–47.3%. However, inconsistent and relatively low decreases by BF in biomass translocation were observed across tillage methods. These results showed that DF increased the wheat yield mainly through promoting biomass production after anthesis. A similar finding was reported by Tong et al. [22]. Additionally, there was a significant and negative relationship between the post-anthesis biomass and biomass translocation in both seasons ($r^2 \geq 0.8248$, $p < 0.05$. Figure 2C), as also shown by Ercoli et al., Duan et al., and Liu et al. [45–47]. This negative relationship indicated a trade-off between the two mass sources in terms of yield contribution. Laza et al. and Nagata et al. stated that the compensatory effect of biomass translocation was always observed when the post-anthesis biomass production was limited by unfavorable conditions, such as low solar radiation, water deficits, and heat stress [44,48]. DF enhanced the water and N supplies for wheat crops after anthesis, resulting in higher production but lower translocation compared to BF. In addition, the biomass translocation was consistently higher in the 2023–2024 season than in the 2022–2023 season. This was because the lower precipitation (44 mm vs. 196 mm) and the higher average maximum temperature (28.5 °C vs. 27.2 °C) during the grain filling limited carbohydrate assimilation. Therefore, the biomass translocation was promoted to compensate for the yield loss due to the unfavorable weather conditions after anthesis in the 2023–2024 season. Breaking the negative relationship between post-anthesis biomass production and biomass translocation, i.e., realizing collaborative improvements in the two grain mass sources may substantially improve the wheat yield by means of optimizing crop management practices or breeding new cultivars in the future.

Biomass is fundamentally driven by two key factors, namely the interception of light and the efficiency with which this intercepted light is converted into biomass, also known as radiation use efficiency (RUE) [24,25,49]. Improving both intercepted solar radiation (ISR) and RUE is critical for maximizing crop biomass and yield [50–52]. DF increased ISR and RUE after anthesis by 12.0–12.4% and 14.4–17.7%, respectively. It indicated that both ISR and RUE played a critical role in enhancing biomass production after anthesis. However,

before anthesis, the increase in RUE (7.7–8.7%) rather than ISR (3.4–4.8%) contributed more to biomass. The greatest response in post-anthesis biomass to DF was achieved for NT, of 36.7–47.3%, followed by RT, of 31.9–32.0%, and PRT of 19.4–21.9%. The collaborative and equal improvements in ISR (16.1–20.7%) and RUE (17.6–19.1%) after anthesis led to the greatest response. GLAI is commonly regarded as a key indicator for assessing a plant's ability to capture and utilize incoming solar radiation [24,27,28,53]. In this study, although DF could increase GLAI after anthesis for all tillage methods, the obvious greatest positive effect was observed under NT in both seasons. Chlorophyll content, i.e., the SPAD value, is typically regarded as a key indicator of RUE [29,30]. High chlorophyll levels generally indicate greater productivity. Our results showed that DF delayed the senescence of leaves and increased the chlorophyll content, thereby significantly improving RUE, especially for NT. In summary, our results highlighted the importance of optimizing water and nitrogen management strategies to maximize yield under conservation tillage.

5. Conclusions

Overall, drip fertigation increased the yield averaged across three tillage methods by 16.8–17.8%, but the yield response to drip fertigation significantly varied among tillage methods. NT performed the highest response, with yields of 2.14–2.16 t ha^{-1} (26.3–28.5%), followed by RT of 1.27–1.35 t ha^{-1} (14.6–15.1%) and PRT of 1.12–1.13 t ha^{-1} (11.0–11.9%). On one hand, the increased ear number per m^2, which mainly came from the greater maximum stems number and grains per ear, contributed to the yield gain by drip fertigation for NT. On the other hand, the substantial increase in post-anthesis biomass (1.99–2.02 t ha^{-1}, i.e., 36.7–47.3%) explained the considerable yield gain. The improved post-anthesis biomass was attributed to both the increased ISR and RUE by drip fertigation after anthesis, which resulted from the promoted GLAI and SPAD, respectively. In addition, the longer post-anthesis duration benefited the biomass. We highlighted that the drip fertigation could make up for the yield sacrifice of NT compared to intensive tillage, i.e., PRT.

Author Contributions: Conceptualization, D.W. and J.X.; methodology, Y.W. and J.S.; software, Y.W. and W.L.; validation, D.W. and J.X.; formal analysis, Y.W., T.Y. and J.X.; investigation, Y.W., J.S. and W.L.; resources, T.Y. and J.S.; data curation, Y.W.; writing—original draft preparation, Y.W. and J.S.; writing—review and editing, D.W., J.X. and Z.G.; visualization, J.X.; supervision, J.X. and Z.G.; project administration, Y.W. and J.X.; funding acquisition, Y.W. and Z.G. All authors have read and agreed to the published version of the manuscript.

Funding: This work was supported by the Ministerial and Provincial Co-Innovation Centre for Endemic Crop Production with High-Quality and Efficiency in Loess Plateau (SBGJXTZX-38); the Shanxi Agricultural University Scientific Research Fund (2020BQ41); the Shanxi University Technological Innovations Plan (2021L171); the Shanxi Fundamental Research Program (202303021222074); and the Shanxi Province Major Science and Technology Special Project (202301140601014-06).

Data Availability Statement: Data are contained within the article.

Conflicts of Interest: The authors declare no conflicts of interest.

References

1. Amo, A.; Serikbay, D.; Song, L.; Chen, L.; Hu, Y. Vernalization and Photoperiod Alleles Greatly Affected Phenological and Agronomic Traits in Bread Wheat under Autumn and Spring Sowing Conditions. *Crop Environ.* **2022**, *1*, 241–250. [CrossRef]
2. Francioni, M.; Palmieri, M.; Fiorentini, M.; Deligios, P.A.; Monaci, E.; Vischetti, C.; Rossa, Ü.B.; Trozzo, L.; Bianchini, M.; Rivosecchi, C.; et al. Scarcity of P-fertilisers: Humic-complexed phosphate as an adaptive solution for wheat and maize under rainfed conditions. *Eur. J. Agron.* **2024**, *156*, 127143. [CrossRef]
3. DeLaune, P.B.; Sij, J.W. Impact of Tillage on Runoff in Long Term No-till Wheat Systems. *Soil Tillage Res.* **2012**, *124*, 32–35. [CrossRef]
4. Nielsen, D.C.; Lyon, D.J.; Hergert, G.W.; Higgins, R.K.; Holman, J.D. Cover Crop Biomass Production and Water Use in the Central Great Plains. *Agron. J.* **2015**, *107*, 2047–2058. [CrossRef]
5. Adil, M.; Lv, F.; Li, T.; Chen, Y.; Gul, I.; Lu, H.; Lu, S.; Qiu, L. Long-Term Effects of Management Practices on Soil Water, Yield and Water Use of Dryland Wheat: A Global Meta-Analysis. *Eur. J. Soil Sci.* **2024**, *75*, e13541. [CrossRef]

6. Chu, P.; Zhang, Y.; Yu, Z.; Guo, Z.; Shi, Y. Winter Wheat Grain Yield, Water Use, Biomass Accumulation and Remobilisation Under Tillage in the North China Plain. *Field Crops Res.* **2016**, *193*, 43–53. [CrossRef]
7. Zhang, Y.; Wang, S.; Wang, H.; Wang, R.; Wang, X.; Li, J. Crop Yield and Soil Properties of Dryland Winter Wheat-Spring Maize Rotation in Response to 10-Year Fertilization and Conservation Tillage Practices on the Loess Plateau. *Field Crops Res.* **2018**, *225*, 170–179. [CrossRef]
8. Ding, J.; Wei, H.; Yang, Y.; Zhang, J.; Wu, J. Effects of Conservation Tillage on Soil Water Condition and Winter Wheat Yield in Farmland. *Chin. J. Appl. Ecol.* **2018**, *29*, 2501–2508. [CrossRef]
9. Wang, X.; Tong, B.; Li, C.; Sun, Z. Influencing Factors of No-Tillage on the Regional Yield of Wheat, Maize, and Rice Using Meta-Analysis. *Trans. CSAE* **2024**, *40*, 133–142. [CrossRef]
10. Chen, T.; Yu, Z.; Shi, Y.; Zhang, Y. Soil Greenhouse Gas Emission and Yield in Wheat Fields under Different Tillage Patterns. *J. Plant Nutr. Fert.* **2023**, *29*, 8–17. [CrossRef]
11. Zhao, K.; Wu, J.; Huang, M.; Li, Y.; Zhao, G.; Fu, G.; Wang, C.; Zhang, Z.; Hou, Y.; Yang, Z. Meta Anlysis of the Effects of Tillange Methods on Grain Yield and Water Use Efficiency in Henan. *J. Triticeae Crops* **2021**, *41*, 891–903. [CrossRef]
12. Chen, J.; Li, S.; Chen, F.; Zhang, H. Characteristic of Accumulated Soil Temperature and Effects on Winter Wheat Under No-Tillage, North Plain, China. *J. Soil Sci.* **2010**, *41*, 547–551. [CrossRef]
13. Jha, S.K.; Gao, Y.; Liu, H.; Huang, Z.; Wang, G.; Liang, Y.; Duan, A. Root Development and Water Uptake in Winter Wheat Under Different Irrigation Methods and Scheduling for North China. *Agric. Water Manag.* **2017**, *182*, 139–150. [CrossRef]
14. Ma, S.; Wang, T.; Ma, S. Effects of Drip Irrigation on Root Activity Pattern, Root-Sourced Signal Characteristics and Yield Stability of Winter Wheat. *Agric. Water Manag.* **2022**, *271*, 107783. [CrossRef]
15. Hagin, J.; Lowengart, A. Fertigation for Minimizing Environmental Pollution by Fertilizers. *Fertil. Res.* **1996**, *43*, 5–7. [CrossRef]
16. Bai, S.; Kang, Y.; Wan, S. Drip Fertigation Regimes for Winter Wheat in the North China Plain. *Agric. Water Manag.* **2020**, *228*, 105885. [CrossRef]
17. Hamani, A.K.M.; Abubakar, S.A.; Si, Z.; Kama, R.; Gao, Y.; Duan, A. Responses of Grain Yield and Water-Nitrogen Dynamic of Drip-Irrigated Winter Wheat (*Triticum aestivum* L.) to Different Nitrogen Fertigation and Water Regimes in the North China Plain. *Agric. Water Manag.* **2023**, *288*, 108494. [CrossRef]
18. Shen, H.; Li, S.; Sun, K.; Gao, Y.; Liu, Y.; Ma, X. Integrated Impacts of Irrigation and Nitrogen Management for Balancing Winter Wheat Yield and Greenhouse Gas Emissions. *Crops Environ.* **2023**, *2*, 126–136. [CrossRef]
19. Si, Z.; Zain, M.; Mehmood, F.; Wang, G.; Gao, Y.; Duan, A. Effects of Nitrogen Application Rate and Irrigation Regime on Growth, Yield, and Water-Nitrogen Use Efficiency of Drip-Irrigated Winter Wheat in the North China Plain. *Agric. Water Manag.* **2020**, *231*, 106002. [CrossRef]
20. Lu, J.; Xiang, Y.; Fan, J.; Zhang, F.; Hu, T. Sustainable High Grain Yield, Nitrogen Use Efficiency and Water Productivity Can Be Achieved in Wheat-Maize Rotation System by Changing Irrigation and Fertilization Strategy. *Agric. Water Manag.* **2021**, *258*, 107177. [CrossRef]
21. Li, H.; Mei, X.; Wang, J.; Huang, F.; Hao, W.; Li, B. Drip Fertigation Significantly Increased Crop Yield, Water Productivity and Nitrogen Use Efficiency with Respect to Traditional Irrigation and Fertilization Practices: A Meta-Analysis in China. *Agric. Water Manag.* **2021**, *244*, 106534. [CrossRef]
22. Tong, J.; Xiong, Y.; Lu, Y.; Li, W.; Lin, W.; Xue, J.; Sun, M.; Wang, Y.; Gao, Z. Drip Fertigation Enhances the Responses of Grain Yield and Quality to Nitrogen Topdressing Rate in Irrigated Winter Wheat in North China. *Plants* **2024**, *13*, 1439. [CrossRef] [PubMed]
23. Ma, S.; Meng, Y.; Han, Q.; Ma, S. Drip Fertilization Improve Water and Nitrogen Use Efficiency by Optimizing Root and Shoot Traits of Winter Wheat. *Front. Plant Sci.* **2023**, *14*, 1201966. [CrossRef] [PubMed]
24. Zhang, Y.; Tang, Q.; Zou, Y.; Li, D.; Qin, J.; Yang, S.; Chen, L.; Xia, B.; Peng, S. Yield Potential and Radiation Use Efficiency of "Super" Hybrid Rice Grown under Subtropical Conditions. *Field Crops Res.* **2009**, *114*, 91–98. [CrossRef]
25. Qin, J.; Impa, S.M.; Tang, Q.; Yang, S.; Yang, J.; Tao, Y.; Jagadish, K.S.V. Integrated Nutrient, Water and Other Agronomic Options to Enhance Rice Grain Yield and N Use Efficiency in Double-Season Rice Crop. *Field Crops Res.* **2013**, *148*, 15–23. [CrossRef]
26. Murchie, E.H.; Burgess, A.J. Casting Light on the Architecture of Crop Yield. *Crops Environ.* **2022**, *1*, 74–85. [CrossRef]
27. Zhu, X.; Long, S.P.; Ort, D.R. Improving Photosynthetic Efficiency for Greater Yield. *Annu. Rev. Plant Biol.* **2010**, *61*, 235–261. [CrossRef] [PubMed]
28. Fletcher, A.L.; Johnstone, P.R.; Chakwizira, E.; Brown, H.E. Radiation Capture and Radiation Use Efficiency in Response to N Supply for Crop Species with Contrasting Canopies. *Field Crops Res.* **2013**, *150*, 126–134. [CrossRef]
29. Kumagai, E.; Araki, A.; Kubota, F. Correlation of Chlorophyll Meter Readings with Gas Exchange and Chlorophyll Fluorescence in Flag Leaves of Rice (*Oryza sativa* L.) Plants. *Plant Prod. Sci.* **2009**, *12*, 50–53. [CrossRef]
30. Huang, M.; Shan, S.; Zhou, X.; Chen, J.; Cao, F.; Jiang, L.; Zou, Y. Leaf Photosynthetic Performance Related to Higher Radiation Use Efficiency and Grain Yield in Hybrid Rice. *Field Crops Res.* **2016**, *193*, 87–93. [CrossRef]
31. Chen, J.; Wang, Y.; Li, H.; Wang, L.; Qiu, J.; Xiao, B. Effects of Drip Fertigation with No-Tillage on Water Use Efficiency and Yield of Winter Wheat. *Acta Agron. Sin.* **2014**, *47*, 1966–1975. [CrossRef]
32. Xue, L.; Khan, S.; Sun, M.; Anwar, S.; Ren, A.; Gao, Z.; Lin, W.; Xue, J.; Yang, Z.; Deng, Y. Effects of Tillage Practices on Water Consumption and Grain Yield of Dryland Winter Wheat Under Different Precipitation Distribution in the Loess Plateau of China. *Soil Tillage Res.* **2019**, *191*, 66–74. [CrossRef]

33. Ye, T.; Ma, J.; Zhang, P.; Shan, S.; Liu, L.; Tang, L.; Cao, W.; Liu, B.; Zhu, Y. Interaction Effects of Irrigation and Nitrogen on the Coordination Between Crop Water Productivity and Nitrogen Use Efficiency in Wheat Production on the North China Plain. *Agric. Water Manag.* **2022**, *271*, 107787. [CrossRef]
34. Wang, W.; Yuan, J.; Gao, S.; Li, T.; Li, Y.; Vinay, N.; Mo, F.; Liao, Y.; Wen, X. Conservation Tillage Enhances Crop Productivity and Decreases Soil Nitrogen Losses in a Rainfed Agroecosystem of the Loess Plateau, China. *J. Clean. Prod.* **2020**, *274*, 122854. [CrossRef]
35. Si, Z.; Qin, A.; Liang, Y.; Duan, A.; Gao, Y. A Review on Regulation of Irrigation Management on Wheat Physiology, Grain Yield, and Quality. *Plants* **2023**, *12*, 692. [CrossRef]
36. Guan, D.; Zhang, Y.; Al-Kaisi, M.M.; Wang, Q.; Zhang, M.; Li, Z. Tillage Practices Effect on Root Distribution and Water Use Efficiency of Winter Wheat under Rain-Fed Condition in the North China Plain. *Soil Tillage Res.* **2015**, *146*, 286–295. [CrossRef]
37. Liu, J.; Fan, Y.; Ma, Y.; Li, Q. Response of Photosynthetic Active Radiation Interception, Dry Matter Accumulation, and Grain Yield to Tillage in Two Winter Wheat Genotypes. *Arch. Agron. Soil Sci.* **2020**, *66*, 1103–1114. [CrossRef]
38. Allard, V.; Martre, P.; Le Gouis, J. Genetic Variability in Biomass Allocation to Roots in Wheat Is Mainly Related to Crop Tillering Dynamics and Nitrogen Status. *Eur. J. Agron.* **2013**, *46*, 68–76. [CrossRef]
39. Zhang, L.; He, X.; Liang, Z.; Zhang, W.; Zou, C.; Chen, X. Tiller Development Affected by Nitrogen Fertilization in a High-yielding Wheat Production System. *Crop Sci.* **2020**, *60*, 1034–1047. [CrossRef]
40. Yang, H.; Xiao, Y.; He, P.; Ai, D.; Zou, Q.; Hu, J.; Liu, Q.; Huang, X.; Zheng, T.; Fan, G. Straw Mulch-Based No-Tillage Improves Tillering Capability of Dryland Wheat by Reducing Asymmetric Competition Between Main Stem and Tillers. *Crop J.* **2022**, *10*, 864–878. [CrossRef]
41. Pheloung, P.; Siddique, K. Contribution of Stem Dry Matter to Grain Yield in Wheat Cultivars. *Funct. Plant Biol.* **1991**, *18*, 53. [CrossRef]
42. Kobata, T.; Palta, J.A.; Turner, N.C. Rate of Development of Postanthesis Water Deficits and Grain Filling of Spring Wheat. *Crop Sci.* **1992**, *32*, 1238–1242. [CrossRef]
43. Yang, J.; Zhang, J.; Huang, Z.; Zhu, Q.; Wang, L. Remobilization of Carbon Reserves Is Improved by Controlled Soil-Drying During Grain Filling of Wheat. *Crop Sci.* **2000**, *40*, 1645–1655. [CrossRef]
44. Laza, M.R.; Peng, S.; Akita, S.; Saka, H. Contribution of Biomass Partitioning and Translocation to Grain Yield Under Sub-Optimum Growing Conditions in Irrigated Rice. *Plant Prod. Sci.* **2003**, *6*, 28–35. [CrossRef]
45. Ercoli, L.; Lulli, L.; Mariotti, M.; Masoni, A.; Arduini, I. Post-Anthesis Dry Matter and Nitrogen Dynamics in Durum Wheat as Affected by Nitrogen Supply and Soil Water Availability. *Eur. J. Agron.* **2008**, *28*, 138–147. [CrossRef]
46. Duan, J.; Wu, Y.; Zhou, Y.; Ren, X.; Shao, Y.; Feng, W.; Zhu, Y.; Wang, Y.; Guo, T. Grain Number Responses to Pre-Anthesis Dry Matter and Nitrogen in Improving Wheat Yield in the Huang-Huai Plain. *Sci. Rep.* **2018**, *8*, 7126. [CrossRef]
47. Liu, M.; Wu, X.; Li, C.; Li, M.; Xiong, T.; Tang, Y. Dry Matter and Nitrogen Accumulation, Partitioning, and Translocation in Synthetic-Derived Wheat Cultivars Under Nitrogen Deficiency at the Post-Jointing Stage. *Field Crops Res.* **2020**, *248*, 107720. [CrossRef]
48. Nagata, K.; Yoshinaga, S.; Takanashi, J.; Terao, T. Effects of Dry Matter Production, Translocation of Nonstructural Carbohydrates and Nitrogen Applicat. *Plant Prod. Sci.* **2001**, *4*, 173–183. [CrossRef]
49. Monteith, J.L.; Moss, C.L. Climate and the Efficiency of Crop Production in Britain. *Phil. Trans. R. Soc. Lond. B* **1977**, *281*, 277–294. [CrossRef]
50. Plénet, D.; Mollier, A.; Pellerin, S. Growth Analysis of Maize Field Crops Under Phosphorus Deficiency. II. Radiation-Use Efficiency, Biomass Accumulation and Yield Components. *Plant Soil* **2000**, *224*, 259–272. [CrossRef]
51. De Costa, W.A.J.M.; Weerakoon, W.M.W.; Herath, H.M.L.K.; Amaratunga, K.S.P.; Abeywardena, R.M.I. Physiology of Yield Determination of Rice Under Elevated Carbon Dioxide at High Temperatures in a Subhumid Tropical Climate. *Field Crops Res.* **2006**, *96*, 336–347. [CrossRef]
52. Reynolds, M.; Foulkes, M.J.; Slafer, G.A.; Berry, P.; Parry, M.A.J.; Snape, J.W.; Angus, W.J. Raising Yield Potential in Wheat. *J. Exp. Bot.* **2009**, *60*, 1899–1918. [CrossRef] [PubMed]
53. Ying, J.; Peng, S.; He, Q.; Yang, H.; Yang, C.; Visperas, R.M.; Cassman, K.G. Comparison of High-Yield Rice in Tropical and Subtropical Environments. *Field Crops Res.* **1998**, *57*, 71–84. [CrossRef]